The magnetic field reconnection site and dissipation region

P. L. Pritchett[1] and F. S. Mozer[2]
[1]*Department of Physics and Astronomy, UCLA, Los Angeles, California 90095-1547, USA*
[2]*Space Sciences Laboratory, University of California, Berkeley, California 94720, USA*

(Received 25 June 2009; accepted 29 July 2009; published online 12 August 2009)

Magnetic field reconnection is said to involve an ion diffusion region surrounding an electron diffusion region. Because of uncertainties in the meanings of these terms and on the physical parameters that characterize them, this paper defines the **reconnection site** as a region having an electron scale size and containing magnetic fields from four topologies, and the **dissipation region**, as having an ion scale size and surrounding the reconnection site. Two-dimensional, asymmetric, open, particle-in-cell simulations, with and without guide fields, examine these regions. It is found that significant values of $(\mathbf{E}+\mathbf{U}_I\times\mathbf{B})$ and/or $(\mathbf{E}+\mathbf{U}_e\times\mathbf{B})$ are not confined to either the reconnection site or the dissipation region. The reconnection site is uninteresting because, for asymmetric reconnection, it does not contain processes that serve to locate it, such as electron acceleration, parallel electric fields, super-Alfvenic electron flow, maximum electron beta, electron nongyrotopy, or demagnetized thermal electrons. However, the surrounding dissipation region exhibits these features. © *2009 American Institute of Physics*. [DOI: 10.1063/1.3206947]

The release of energy stored in stressed magnetic fields via magnetic reconnection is a fundamental plasma process that occurs in systems possessing magnetic shear.[1–3] Sawteeth and disruptions in tokamaks, substorms in the terrestrial magnetosphere, flares in the solar corona, astrophysical gamma-ray bursts, and magnetically striped relativistic winds are among the many phenomena that may involve reconnection in the dissipation process. The fundamental physics that powers these effects arises in a narrow layer where collisionless dissipation enables the change in magnetic field topology.

The conventional description of the dissipation region in collisionless magnetic reconnection involves a two-scale structure.[4,5] The larger structure, often called the ion diffusion region, has a size $\sim c/\omega_{\mathrm{pI}}$, where ω_{pI} is the ion plasma frequency. The smaller structure, often called the electron diffusion region, is embedded in the larger structure and has a size $\sim c/\omega_{\mathrm{pe}}$, where ω_{pe} is the electron plasma frequency. The ions and electrons are said to be unmagnetized [which may mean that $(\mathbf{E}+\mathbf{U}_I\times\mathbf{B})\neq 0$ and $(\mathbf{E}+\mathbf{U}_e\times\mathbf{B})\neq 0$, where $\mathbf{U}_I$ and $\mathbf{U}_e$ are the ion and electron bulk flows and $\mathbf{E}$ and $\mathbf{B}$ are the electric and magnetic fields] in the larger and smaller regions, respectively, and the reconnection physics occurs in the smaller region.

Because there is no general agreement on the definitions of these two regions or on the physical parameters that characterize them, this paper defines alternative but related concepts of the **reconnection site** and the **dissipation region**. The reconnection site is the volume within which four different classes of magnetic fields reside. For subsolar magnetospheric reconnection at the terrestrial magnetopause, these four classes are magnetospheric field lines, magnetosheath field lines, reconnected field lines above the *X*-line, and reconnected field lines below the *X*-line. For two-dimensional (2D) reconnection, the reconnection site has dimensions $\sim c/\omega_{\mathrm{pe}}$ in the direction perpendicular to the current sheet (the *X*-direction) and the direction parallel to the plasma outflow (the *Z*-direction), and is elongated in the *Y*-direction to contain the *X*-line. The dissipation region, of size $\sim c/\omega_{\mathrm{pI}}$, is that region around the reconnection site where significant electromagnetic energy conversion occurs.

Phenomena that might be useful for identifying the reconnection site include a nonzero parallel electric field, $\mathbf{E}_{\|}$, electron acceleration, electromagnetic energy conversion, a large perpendicular electric field, super-Alfvenic electron outflow, nongyrotropy of the electron distribution, demagnetization of thermal electrons, a filamentary current channel, a rapid density variation, etc. There is no consensus on which of these proxies is most suitable for representing the reconnection site.[6–9]

In this paper, the reconnection site is identified from the magnetic field topology. Then, results from 2D particle-in-cell simulations with a grid size of $\sim 0.3\ c/\omega_{\mathrm{pe}}$ and open boundary conditions for asymmetric reconnection with and without a guide field[10] are used to test how well the various proxies select the reconnection site or dissipation region. The ion to electron mass ratio in the simulations is 200. The density drops by a factor of 10 across the current layer (from the magnetosheath to the magnetosphere for subsolar reconnection), and the strength of the reversing magnetic field increases by a factor of 3. The asymmetric case is the most prevalent form of reconnection at the subsolar magnetosphere, at the sun, and in all of astrophysics. In addition, this case removes many of the symmetry constraints that may limit the generality of the more common symmetric analyses of reconnection. It will be shown that the reconnection site is an uninteresting locale because it is a singularity and that the interesting physics occurs in the larger dissipation region around it.

A necessary condition for reconnection is found by considering magnetic field line motion. Field lines moving with the $\mathbf{E}\times\mathbf{B}/B^2$ velocity produce the same temporal evolution

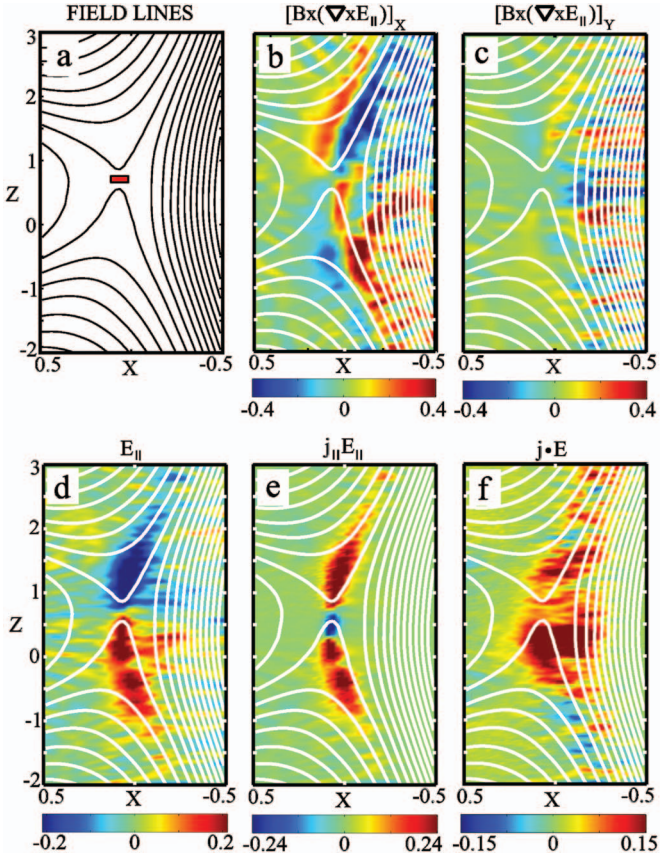

FIG. 1. (Color) Topologies of fields and related quantities for asymmetric reconnection with no guide field. Note that the color scales in all panels are saturated at half the maximum absolute value of the quantity of interest.

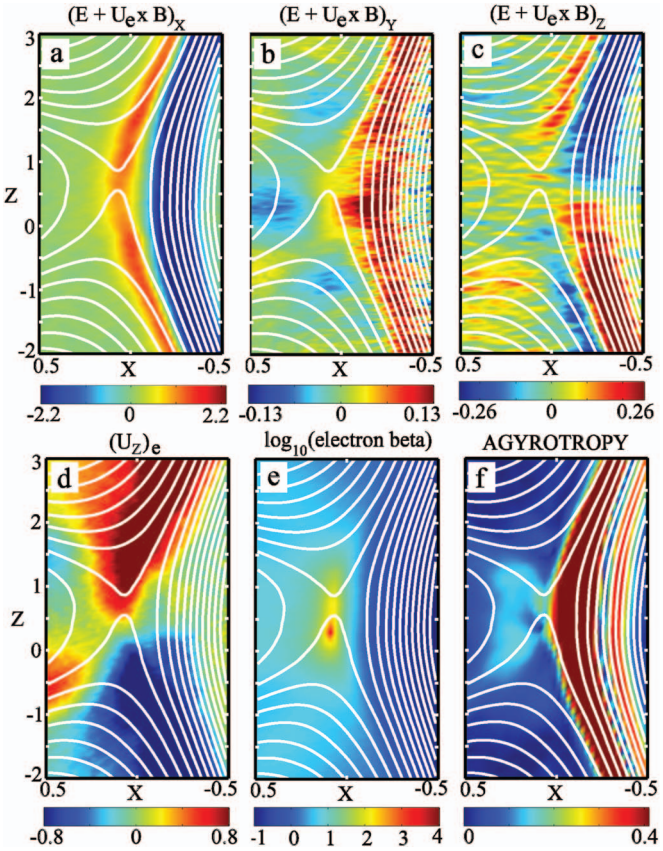

FIG. 2. (Color) Topologies of parameters that might serve as proxies for locating the reconnection site for asymmetric reconnection with no guide field.

of the magnetic field as do Maxwell's equations if[6,11,12]

$$\mathbf{B} \times (\nabla \times \mathbf{E}_{\|}) = 0. \tag{1}$$

When this equation is satisfied, the evolution of the magnetic field topology may be visualized as due to field lines moving at the $\mathbf{E}\times\mathbf{B}/B^2$ velocity. In this case, a pair of oppositely directed field lines, moving toward each other in the presence of a perpendicular electric field, would pass through one another without reconnecting. Because this result is nonphysical, Eq. (1) must not be satisfied at the reconnection site. This is a necessary but not sufficient condition for reconnection because failure to satisfy Eq. (1) means only that the magnetic field evolution must be determined by solving Maxwell's equations.

Panel (a) of Fig. 1 gives the magnetic field topology for the asymmetric simulation with no guide field at a time $\Omega_{oI}t=65$. This simulation is initialized with an X-line perturbation and the total system size is $L_X\times L_Z=25.6\ c/\omega_{pI}\times 51.2\ c/\omega_{pI}$. The spatial scale of all panels in all figures is c/ω_{pI} in X and 5 c/ω_{pI} in Z. The red box in panel (a), with dimensions of c/ω_{pe} by c/ω_{pe}, is the reconnection site because the four classes of magnetic field lines thread through it. For clarity, these four field lines are not illustrated.

The X- and Y-components of the left side of Eq. (1) are given in panels (b) and (c) of Fig. 1 (the Z-component is not shown because it is nearly an order-of-magnitude smaller). In these and all panels in all figures, other than those panels specifically excluded, the color scales are saturated at half the maximum absolute value of the quantity of interest such that the red and blue regions include values that are within a factor of 2 of the maximum. Because of the significant values of the components of Eq. (1) in panels (b) and (c), it is incorrect to attempt to visualize field line motion at the $\mathbf{E}\times\mathbf{B}/B^2$ velocity over large regions surrounding the reconnection site.

The parallel electric field of panel (d) is significant over X-distances of a few c/ω_{pe} and Z-distances of $\sim 4\ c/\omega_{pI}$. This is consistent with the frequent observations of such fields in space.[6] While these parallel electric fields are not associated with the reconnection site, they are associated with the interesting physics of the dissipation region.

Panels (e) and (f) give $j_{\|}E_{\|}$, the part of $\mathbf{j}\cdot\mathbf{E}$ associated with the parallel electric field, and the total value of $\mathbf{j}\cdot\mathbf{E}$. While $j_{\|}E_{\|}$ is largely confined to the dissipation region, total energy conversion occurs over a wider region in X and along the separatricies (not shown). Little energy conversion occurs in the reconnection site. Within the dissipation region, the energy conversion and acceleration involve mainly the electrons because their flow speeds exceed those of ions by a factor ~ 5.

The three components of $(\mathbf{E}+\mathbf{U}_e\times\mathbf{B})$ are given in panels (a), (b), and (c) of Fig. 2. The X-component is nearly an order-of-magnitude larger than the other components, and none of them serve to locate uniquely either the reconnection

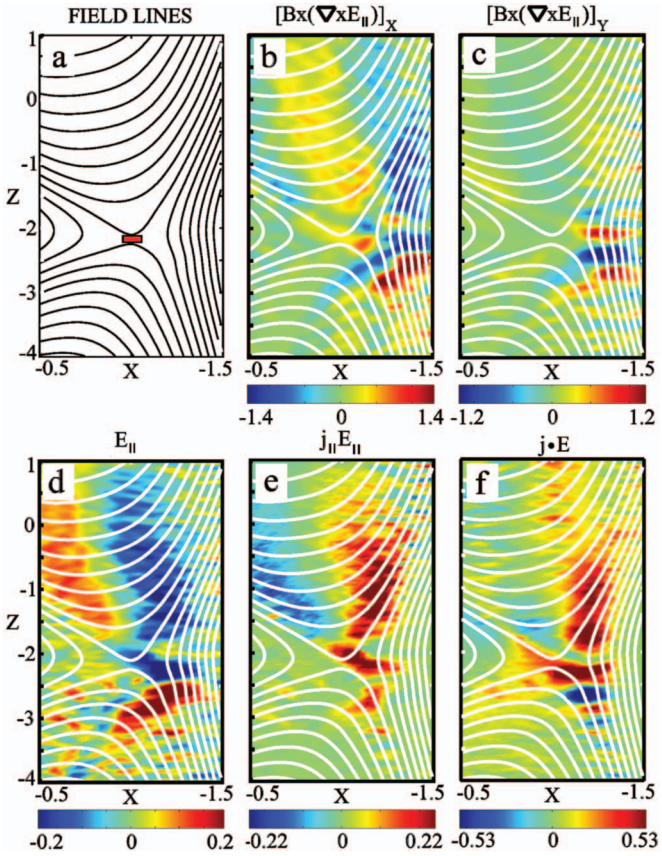

FIG. 3. (Color) Topologies of fields and related quantities for asymmetric reconnection with a guide field. Note that the color scales in all panels are saturated at half the maximum absolute value of the quantity of interest.

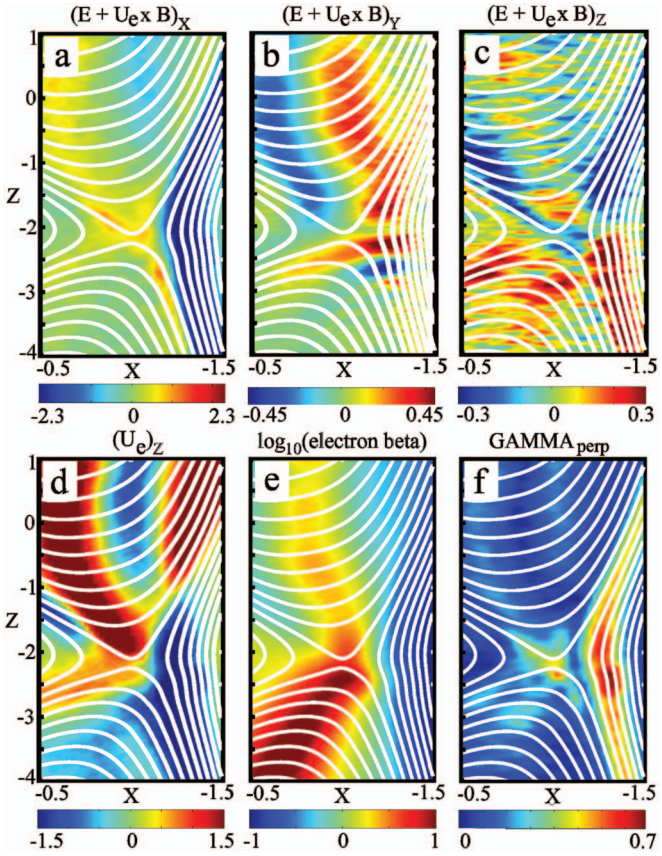

FIG. 4. (Color) Topologies of parameters that might serve as proxies for locating the reconnection site for asymmetric reconnection with a guide field.

site or the dissipation region. Instead, $(\mathbf{E}+\mathbf{U}_e\times\mathbf{B})$ is most useful for painting the magnetospheric separatrix.

Panel (d) of Fig. 2 gives the electron outflow in the Z-direction. The electrons are weakly accelerated at the reconnection site, but they gain a velocity up to 2–3 times the Alfven speed in the dissipation region.

The electron beta is plotted in panel (e) of Fig. 2 in a color scale that covers its dynamic range. While beta is greater than one at the reconnection site, its value in the nearby dissipation region is a factor of ~30 greater. Thus, multiple spacecraft crossing the subsolar magnetopause would mislocate the reconnection site by a fraction of an ion skin depth if they identified it with the maximum of the electron beta. It is noted that beta at the reconnection site is less than 100 for the case of no guide field (and less than 10 for the guide field case, as discussed below), which means that the magnetic field does not go to zero at the reconnection site in spite of the fact that the in-plane component does go to zero at this location.

The agyrotropy of the electron pitch angle distribution[7] is given in panel (f) of Fig. 2. It does not locate either the reconnection site or the dissipation region, and it has appreciable values only along the magnetospheric separatrix.

Figures 3 and 4 give results for the case of a guide magnetic field equal to the magnetosheath reconnecting field. This simulation was driven by an external E_Y field imposed at the magnetosheath boundary and the total system size was $L_X\times L_Z=25.6\ c/\omega_{pI}\times 25.6\ c/\omega_{pI}$. Panel (a) of Fig. 3 gives the in-plane magnetic field geometry for this case at a simulation time of $\Omega_{oI}t=72.5$. Two components of $\mathbf{B}\times(\nabla\times\mathbf{E}_{\|})$, in panels (b) and (c), are nonzero over large regions. The dissipation region, evidenced by the data in panels (d), (e), and (f) of Fig. 3, is distorted from that associated with the simpler case of no guide field, and $\mathbf{j}\cdot\mathbf{E}$ is greater than $j_{\|}E_{\|}$ in the vicinity of the reconnection site.

Panels (a), (b), and (c) of Fig. 4 give the three components of $(\mathbf{E}+\mathbf{U}_e\times\mathbf{B})$. As was the case in Fig. 2, the nonzero regions in these panels give little information on the location of the reconnection site. Even so, the spatial distribution of the nonzero values of $(\mathbf{E}+\mathbf{U}_e\times\mathbf{B})_Y$ are similar to that for $E_{\|}$ and $j_{\|}E_{\|}$ given in Fig. 3 so this parameter does characterize the dissipation region for the guide field case, but not for the case of no guide field.

Panel (d) of Fig. 4 gives the electron outflow speed, which is mainly along the separatricies, except that there is an additional northward flow through the center of the current sheet that commences in the dissipation region just outside the reconnection site. The electron beta of panel (e) in Fig. 4, plotted with a color scale that covers its dynamic range, is greater than one at the reconnection site, but it is larger than that over an extensive region south of the site.

It has been speculated that the reconnection site can be identified as the location where thermal electrons are demagnetized such that the perpendicular Lorentz ratio, gamma, is

comparable to or greater than one.[7] To test this possibility, gamma is presented in panel (f) of Fig. 4 in a color scale that covers its dynamic range. While gamma has a local maximum in the dissipation region, it is comparable to one only along the magnetospheric separatrix. Thus, thermal electrons are not demagnetized at the reconnection site or in the dissipation region according to this criterion. For no guide field, gamma is greater than one at the reconnection site but it is even larger in the dissipation region. Thus, even for this case, the proposed criterion does not uniquely determine the reconnection site.

In summary, the reconnection site associated with magnetic field reconnection is defined as the region having planar dimensions the order of the electron skin depth and within which magnetic fields from four different topologies reside. The dissipation region is identified as the location around the reconnection site where important conversion of electromagnetic energy occurs. For reconnection with and without a guide magnetic field, the geometries of these regions differ. However, in both cases, significant electromagnetic energy conversion is not found within the reconnection site, as are none of the processes that have been mentioned in the literature as being associated with this site. In particular, locations where $(\mathbf{E}+\mathbf{U}_e\times\mathbf{B})$ is nonzero cover areas much larger than the reconnection site. The maximum value of the electron beta lies within the dissipation region but outside the reconnection site. The electron acceleration also occurs in the dissipation region. The demagnetization of thermal electrons and the nongyrotropy of the electron distribution do not provide useful proxies for finding the reconnection site or dissipation region. Significant parallel electric fields and electromagnetic energy conversion exist in a region where reconnection cannot occur. Thus, significant electric fields and electromagnetic energy conversion do not occur at the reconnection site while these interesting and significant features exist where reconnection cannot happen. Thus, no physically interesting parameter or combination of parameters serves to characterize the reconnection site and it may only be found from the magnetic field topology, which is difficult to measure in space. Lastly, because there are regions on the ion scale where $\mathbf{B}\times(\nabla\times\mathbf{E}_{\|})\neq 0$, the correct magnetic field configuration cannot be obtained by propagating field lines at $\mathbf{E}\times\mathbf{B}/B^2$ over such very large regions.

This research was supported by NASA Grant Nos. NNX08AM15G, NNG05GL27G, and NNG05GC72G and Contract No. NAS5-02099-07/09. The particle simulations were performed using resources of the San Diego Supercomputer Center (supported by the National Science Foundation under Cooperative Agreement No. ACI-9619020) and the UCLA Dawson Cluster (funded by NSF Grant No. PHY-0321345).

[1] V. M. Vasyliunas, Rev. Geophys. **13**, 303, DOI: 10.1029/RG013i001p00303 (1975).
[2] B. U. O. Sonnerup, in *Solar System Plasma Physics*, edited by L. T. Lanzerotti, C. F. Kennel, and E. N. Parker (North-Holland, New York, 1979), Vol. 3, p. 45.
[3] A. A. Galeev, in *Basic Plasma Physics*, edited by A. A. Galeev and R. N. Sudan (North-Holland, New York, 1984), Vol. 2, p. 305.
[4] D. Biskamp, E. Schwarz, and J. F. Drake, Phys. Plasmas **4**, 1002 (1997).
[5] J. F. Drake and M. A. Shay, in *Reconnection of Magnetic Fields*, edited by J. Birn and E. R. Priest (Cambridge University Press, Cambridge, 2007), Sec. 3.1.
[6] F. S. Mozer, J. Geophys. Res. **110**, A12222, DOI: 10.1029/2005JA011258 (2005).
[7] J. D. Scudder, R. D. Holdaway, R. Glassberg, and S. L. Rodriguez, J. Geophys. Res. **113**, A10208, DOI: 10.1029/2008JA013361 (2008).
[8] M. A. Shay, J. F. Drake, and M. Swisdak, Phys. Rev. Lett. **99**, 155002 (2007).
[9] H. Ji, Y. Ren, M. Yamada, S. Dorfman, W. Daughton, and S. P. Gerhardt, Geophys. Res. Lett. **35**, L13106, DOI: 10.1029/2008GL034538 (2008).
[10] P. L. Pritchett, J. Geophys. Res. **113**, A06210, DOI: 10.1029/2007JA012930 (2008).
[11] W. A. Newcomb, Ann. Phys. **3**, 347 (1958).
[12] C. L. Longmire, *Elementary Plasma Physics* (Wiley, New York, 1963).